

# Causes of decreased reference evapotranspiration and pan evaporation in the Jinghe River catchment, northern China

Pei Wang · Tsutomu Yamanaka · Guo Yu Qiu

Published online: 15 November 2011  
© Springer Science+Business Media, LLC 2011

**Abstract** This study focused on the changes of reference evapotranspiration ( $ET_0$ ) and pan evaporation ( $ET_{pan}$ ) to study the impacts of climate change on the hydrological cycle in the Jinghe River catchment. Based on the Penman–Monteith equation, the  $ET_0$  was calculated. The temporal trend and spatial distribution of  $ET_0$  and  $E_{pan}$  measured with a 20-cm pan were examined at the 14 stations during 1957–2005. The effects of meteorological factors on the variation of  $ET_0$  were determined by analyzing the trends in themselves with comparison between original climate and detrended climate scenarios and then their sensitivity to  $ET_0$ . Both the  $ET_0$  and  $E_{pan}$  showed remarkable decreasing trends from 1957 to 2005 and their decreasing rate was 40.9 and 17.7 mm per 10 years, respectively. Trend analysis of meteorological factors exhibited that the reduction in  $ET_0$  and  $ET_{pan}$  was principally caused by both significant decreases in wind speed and sunshine hours. Furthermore, the decreasing trend of  $ET_0$  was mainly dominated by the significant decrease in wind speed with high sensitivity, to a less extent, by the decrease in net radiation. Although relative humidity is one of the most sensitive variables, its effect on  $ET_0$  was negligible because of its temporal constancy. The

contribution of wind speed reduction to decreased  $ET_0$  has increased from 50 to 76.1%, but net radiation, by contrast, decreased from 50 to 23.9%.

**Keywords** Reference evapotranspiration · Pan evaporation · Trend analysis · Jinghe River catchment · Northern China

## Abbreviations

$ET_0$	Reference evapotranspiration
$E_{pan}$	Pan evaporation
DTR	Diurnal temperature range
SA	Sensitivity analysis
$e_a$	Actual vapor pressure
$e_s$	Saturated vapor pressure
DFA	Detrended fluctuation analysis
VPD	Vapor pressure deficit
$T_{max}$	Average annual maximum temperature
$R_n$	Net solar radiation
$T_{min}$	Average annual minimum temperature
FAO	Food and Agricultural Organization

P. Wang (✉)  
Graduate School of Life and Environmental Sciences,  
University of Tsukuba, Tsukuba 305-8577, Japan  
e-mail: wangpei@geoenv.tsukuba.ac.jp

T. Yamanaka  
Terrestrial Environment Research Center, University  
of Tsukuba, Tsukuba 305-8577, Japan

G. Y. Qiu  
Key Laboratory for Urban Habitat Environment Science and  
Technology, School of Environment and Energy, Shenzhen  
Graduate School of Peking University, Shenzhen 518055, China

## 1 Introduction

Climate change results from global warming have had a great impact on evaporation and hence the hydrology cycle. Evapotranspiration is an important component of hydrologic cycle and influence the availability of water, particularly for agriculture (Burn and Hesch 2007). Reference evapotranspiration ( $ET_0$ ) serves as a vital parameter for many aspects, such as water resources planning, irrigation management, and hydrological modeling. It is

critical to understand the responding mechanism of  $ET_0$  to the climate changes for regional hydrological studies and water resource planning for high water-use efficiency.

Several methods exist to estimate the reference evapotranspiration (Sumner and Jacobs 2005; Xu and Singh 2000, 2001). These methods are based on meteorological factors, such as air temperature (Thornthwaite 1948), solar radiation (Turc 1961), or other factors, such as mass transfer (Harbeck 1962) or some measurement related to these variables, like pan evaporation, and these methods were developed for specific studies and most of them are more apt to use in climate-similar areas. The Penman–Monteith method approach was recommended by FAO (Allen et al. 1998) as a sole standard method to calculate reference evapotranspiration wherever the required data were available. Pan evaporation is also often used to estimate reference evapotranspiration. The evaporation rate from pans filled with water provides an index of the integrated effect of radiation, air temperature, air humidity, and wind on evapotranspiration, which is a good proxy for estimating the  $ET_0$ . Although the pan responds in a similar fashion to the same climatic factors affecting crop transpiration, several factors produce significant differences in loss of water from a water surface and from a cropped surface. The pan has proven its practical value and has been used successfully to estimate  $ET_0$  by observing the evaporation loss from a water surface and applying empirical coefficients to relate pan evaporation to  $ET_0$  (Allen et al. 1998).

There are already several reports about the decreasing trends of reference evapotranspiration in China. The trend is more likely caused by decreased sunshine duration over China (Kaiser and Qian 2002) that may be related to increases in air pollution and atmospheric aerosols (Liepert et al. 2004) and increases in cloud cover (Dai et al. 1999) and decreased wind speed (Yin et al. 2009). In ChangJiang catchment, by the decrease in net radiation and wind speed (Xu et al. 2006). Over the Tibetan Plateau (Shenbin et al. 2006), wind speed and relative humidity were found to be the most important meteorological variables affecting  $ET_0$  trends. In addition, there are many worldwide reports about the decreasing trends of pan evaporation over the USA (Peterson et al. 1995; Golubev et al. 2001; Hobbins et al. 2004), India (Chattopadhyay and Hulme 1997), Australia (Roderick and Farquhar 2004), New Zealand (Roderick and Farquhar 2005), China (Yin et al. 2009), and Thailand (Tebakari et al. 2005). The trend is more likely caused by decreasing surface solar radiation over the USA and parts of Europe and Russia (Abakumova et al. 1996; Liepert 2002) and decreased sunshine duration over China (Kaiser and Qian 2002) that may be related to increases in air pollution and atmospheric aerosols (Liepert et al. 2004; Qian et al. 2006) and increases in cloud cover (Dai et al.

1999) and decreased wind speed (Yin et al. 2009). Moreover, for changes in the observed pan evaporation over the Yellow River basin, Liu and Zeng (2004) pointed out that the decrease of pan evaporation is mainly related to reductions of solar irradiance, owing to more clouds and aerosols.

The Jinghe River watershed, a tributary of the Yellow River covering the central region of the Loess Plateau, is one of the most vulnerable areas of the process of aridification in northern China. In the past 50 years, the mean annual precipitation, actual evapotranspiration, and runoff have had an obvious reduction (Qiu et al. 2008), which increased the water stress, combined with increased water demand. Changes of reference evapotranspiration in this region could have a substantial economic impact due to the importance to agriculture activity. The identification and quantification of evapotranspiration will provide insight into the future water balance in the Jinghe River watershed and facilitate improved water resource management for the region.

However, many previous studies have been carried out on a larger scale, e.g., a national scale (Kaiser and Qian 2002; Yin et al. 2009) and Yellow River watershed (Liu and Zeng 2004; Liu et al. 2010), which is too coarse to apply in Jinghe River watershed. In addition to these aspects, most of the studies conducted in the Yellow River watershed only described climate factors have positive or negative effects on  $ET_0$ ; they had no further quantitative analyses. Since the processes driving changes on  $ET_0$  over Jinghe River watershed are still unclear, it is necessary to evaluate and quantify them. Therefore, the objectives of this study are (1) to investigate the trends of  $ET_0$  and  $ET_{pan}$  in Jinghe River watershed, (2) to identify the driving factors attributed to changes to  $ET_0$  and  $ET_{pan}$ , and (3) to quantify the dynamic contributions on changes of  $ET_0$ .

## 2 Materials and methods

### 2.1 Research area and data processing

Jinghe River catchment lies in the middle and upper reaches of the Yellow River and is characterized by climate transition zone from the arid region to the humid region, including 31 counties and cities in northern China and covers an area of approximately 45,421 km<sup>2</sup>. Administrative boundaries are within 105°49′–108°58′E and 34°14′–38°10′N, and average about 1,200 m above mean sea level. The topography of the watershed is high in the northern part and low in the southern part, with Liupan Mountain on the west side and Ziwu Mountain on the east side. Jinghe River and its tributaries all cut deeply into the loess landscape (Fig. 1). Temperature in the basin ranges from high

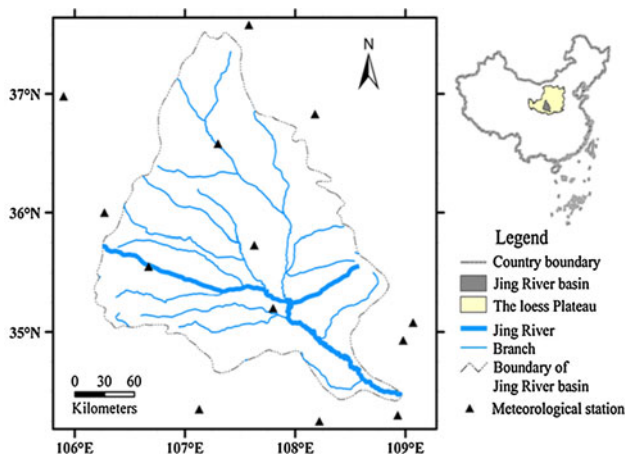


**Fig. 1** Geographical locations of the Jinghe River watershed and national meteorological stations in northern China

in the south to low in the north, with annual mean temperature of 8–13°C. Annual frost-free period is about 150–210 days. The annual average precipitation is about 550 mm during past 50 years, and varies from 100 mm in the north to 700 mm in the south. The annual average pan evaporation is about 1,656 mm during 1957–2005, and gradually decreases from north to south, as shown in Table 1. The whole basin was divided into three sub-regions from south to north as follows: an arid region, (precipitation < 400 mm), a sub-arid and sub-humid region (precipitation ranges between 400 and 600 mm), and a humid region (precipitation > 600 mm).

Data of 14 national meteorological stations with daily observations of maximum, minimum, and mean (near the surface) air temperature, wind speed, sunshine hours,

relative humidity, and pan evaporation of 20 cm diameter pans from 1957 to 2005 were used In this study (Table 1), provided by the National Climatic Center (NCC) of China Meteorological Administration (CMA). Before analysis, we carried out data quality control with the following procedures: (1) from the entire 1957–2005 period, data must be available for at least 45 years; (2) missing data cannot be more than 10%; (3) missing data from each year cannot exceed 20%.

### 2.2 Estimation of the reference evapotranspiration

The Penman–Monteith method (P–M method) is recommended as the sole method for determining  $ET_0$  by FAO (Allen et al. 1998), and it is also used in this study (Eq. 1). The method is selected because it is physically based and explicitly incorporates both the physiological and aerodynamic parameter.

$$ET_0 = \frac{0.408 \Delta (R_n - G) + \gamma \frac{900}{T+273} U_2 (e_a - e_s)}{\Delta + \gamma (1 + 0.34 U_2)}, \quad (1)$$

where  $ET_0$  is the reference evapotranspiration ( $\text{mm day}^{-1}$ ),  $R_n$  the net radiation at the crop surface ( $\text{MJ m}^{-2} \text{day}^{-1}$ ),  $G$  the soil heat flux density ( $\text{MJ m}^{-2} \text{day}^{-1}$ ),  $T$  the mean daily air temperature at 2 m height ( $^{\circ}\text{C}$ ),  $u_2$  the wind speed at 2 m height ( $\text{m s}^{-1}$ ),  $e_s$  the saturation vapor pressure ( $\text{kPa}$ ),  $e_a$  the actual vapor pressure ( $\text{kPa}$ ),  $e_s - e_a$  the saturation vapor pressure deficit ( $\text{kPa}$ ),  $\Delta$  the slope vapor pressure curve ( $\text{kPa } ^{\circ}\text{C}^{-1}$ ),  $\gamma$  is psychrometric constant ( $\text{kPa } ^{\circ}\text{C}^{-1}$ ).

According to Allen et al.’s (1998) produce to estimate  $ET_0$ , the global solar radiation can be estimate by the Angstrom-Preccott (Preccott 1940), which can be expressed as:

**Table 1** Information of meteorological stations used in the Jinghe River watershed

Subregion	Mean annual precipitation (1957–2005)	ID	Station	Belongs to	N. Lat	E. Long	<i>m</i>
Arid region	$P \ll 400 \text{ mm}$	53,810	Tong Xin	Ning Xia	36°58''	105°54''	1,339.3
		53,723	Yan Chi	Ning Xia	37°48'	107°23''	1,349.3
		53,740	Zhong Ning	Ning Xia	37°29''	105°4''	1,185.0
Sub-arid and sub-humid region	$400 \text{ mm} < p < 600 \text{ mm}$	53,817	Gu Yuan	Ning Xia	36°00''	106°16''	1,753.0
		53,821	Huan Xian	Gan Su	36°35''	107°18''	1,255.6
		53,903	Xi Ji	Ning Xia	35°58''	105°43''	1,916.5
		53,915	Ping Liang	Gan Su	35°33''	106°40''	1,346.6
		53,923	Xi Fenzhen	Gan Su	35°44''	107°38''	1,421.0
		53,929	Chuan Wu	Shang Xi	35°12''	107°48''	1,206.5
		53,738	Wu Qi	Shan Xi	36°55''	108°10''	1,331.4
Humid region	$P \gg 600 \text{ mm}$	53,942	Luo Chuan	Shang Xi	35°49''	109°30''	1,159.8
		57,034	Wu Gong	Shang Xi	34°15''	108°13''	449.1
		57,036	Xi An	Shang Xi	34°18''	108°56''	398.6
		57,016	Bao Ji	Shang Xi	34°21''	107°08''	613.6

$$R_s = \left( a + b \frac{n}{N} \right) R_a, \quad (2)$$

where  $R_a$  is extra-terrestrial solar radiation ( $\text{MJ m}^2 \text{d}^{-1}$ ),  $n$  is actual sunshine hour and  $N$  is potential sunshine hours,  $a$  and  $b$  are regression constants. According to Chen et al. (2004),  $a$  and  $b$  were set to 0.19 and 0.53, respectively, in this study.

### 2.3 Temporal analysis

The conventional least-squares fitting method is used to estimate the magnitude of climate changes in terms of linear trend. Significance of the trend was tested both by parameter  $T$  test and non-parameter Mann–Kendall statistical test (Kendall 1975; Mann 1945). Parameter  $T$  test comprises two steps, fitting a liner simple regression equation with time  $t$  as an independent parameter and meteorological variables,  $Y$  as dependent variables, (in this case  $\text{ET}_0$  or  $\text{ET}_{\text{pan}}$ ), then testing the equation, statistical significance of the slope of the regression equation. The Mann–Kendall test is a non-parametric test for identified trends in time series data, a test to compare the relative magnitudes of data rather than the data values themselves. The principle is testing the significance of the Mann–Kendall statistic (Kendall's tau) and the procedure is present in many standard statistics books (Helsel and Hirsch 1993).

### 2.4 Detrended method

The detrended fluctuation analysis method (DFA) (Bunde et al. 2000; Kantelhardt et al. 2001; Koscielny-Bunde et al. 2006) was widely used to eliminate the influence of possible trends existing in the variables (Koscielny-Bunde et al. 2006). There are different orders of DFA that are distinguished by removed trends in the data. In the lowest order, we determine the best linear fit (DFA1) of the time series. DFA1 computes the least-squares fit of a straight line to the data and subtracts the resulting function from the data. For example,  $Y = \text{DFA1}(x)$  removes the straight-line fit from time series  $x$  and returns it in time series  $Y$ .

### 2.5 Sensitivity analysis

Sensitivity analysis of  $\text{ET}_0$  to the meteorological variables is performed by calculating the input variables (relative changes of each variables) against the resultant change (relative changes of  $\text{ET}_0$ ) as a crave (i.e., sensitivity crave). Compared to other methods (Gong et al. 2006; Qiu et al. 1998), this method is simple and practical and used by many authors (Paturol et al. 1995; Xu and Vandewiele 1994).

## 3 Results

### 3.1 Long-term variation trends of reference evapotranspiration and pan evaporation and their spatial distribution

Figure 3 shows that a decreasing trend is clearly detected for  $\text{ET}_0$  and  $\text{ET}_{\text{pan}}$ . In order to test the significance of the trend in  $\text{ET}_0$  and  $\text{ET}_{\text{pan}}$  time series, both parametric  $t$  test and non-parametric Mann–Kendall test are conducted. Results of trend analysis of the  $\text{ET}_0$  and  $\text{ET}_{\text{pan}}$  are shown in Table 3 (row 1 and row 2). It is seen that the hypothesis of no trend is rejected in both the  $T$  test and Mann–Kendall test. In other words, the decreasing trend is significant at the 5% significance level. The spatial distribution of annual reference evapotranspiration and pan evaporation's trend coefficients are plotted in Fig. 2. Circles and squares indicate the decreasing and increasing tendencies, respectively, while the circles and squares size to indicate the intensity of those positive or negative trends. As it can be seen, among 14 stations, that 12 stations show decreasing trend in  $\text{ET}_0$  except Xi'An and Bao'Ji stations (Humid region). Detailed tendency analysis of trend coefficients of pan evaporation is presented in Fig. 2; pan evaporation had almost similar trends to  $\text{ET}_0$ . The decreased tendency of pan evaporation is detected in the last 49 years.

For the whole watershed, the  $\text{ET}_0$  has decreased significantly (at the 95% level of confidence), averaged change ratios of  $-17.7$  mm per 10 years; the pan evaporation had larger trends than the reference evapotranspiration. The change ratios reached  $-40.6$  mm per 10 years (Fig. 3; Table 3). The changes of pan evaporation were higher than the national average rate of  $-34$  mm per 10 years reported by the Compilation Commission of China's National Assessment for Climate Change (2007).

### 3.2 Trend analysis of meteorological factors

The temporal trend detected in  $\text{E}_{\text{pan}}$  and  $\text{ET}_0$  reveals a combined effect of all meteorological variables. In order to detect the cause of decreased  $\text{ET}_0$  and  $\text{E}_{\text{pan}}$ , the same trend analysis procedure for the main meteorological variables that determined the magnitude of  $\text{ET}_0$  are preformed, the meteorological variables that are examined including maximum temperature ( $T_{\text{max}}$ ) and minimum temperature ( $T_{\text{min}}$ ), relative humid (RH), wind speed, and sunshine hours. In addition, the combined variables such as vapor pressure deficit (VPD) and diurnal temperature range (DTR) are also tested.

As shown in Table 2, the  $\text{ET}_0$  was negatively closed to the relative humidity and positive to others. That is, all variables, except relative humidity, have a positive effect



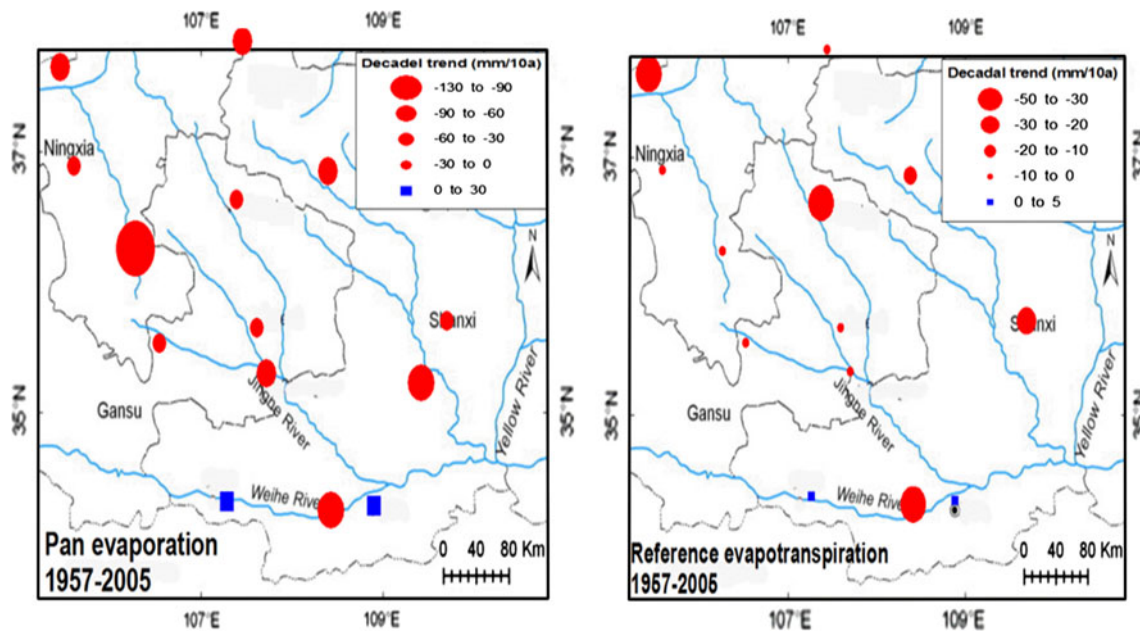


**Fig. 2** Linear trends ( $^{\circ}\text{C}/\text{decade}^{-1}$ ) in pan evaporation and reference evapotranspiration from 1957 to 2005 over the Jinghe River watershed based on 14 stations (dots)

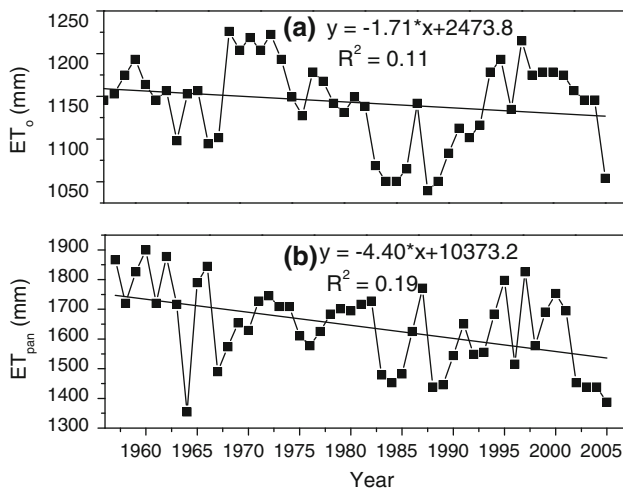


**Fig. 3** Linear trend ( $^{\circ}\text{C}/\text{decade}^{-1}$ ) in reference evapotranspiration (a) and pan evaporation (b) from 1957 to 2005 over Jinghe River watershed based on 14 stations (dots), northern China. Dot size is related to linear trend

on  $ET_0$ . Moreover, the  $E_{pan}$  and  $ET_0$  almost have the same correlation of meteorological variables.

The results of trend analysis of the meteorological variables are shown in Table 3 and Fig. 4. It is of note that both tests show that two out of seven variables, i.e., wind speed and sunshine hours have a significantly declined trend over the past 49 years, which causes negative effects of the changes of  $ET_0$  and  $E_{pan}$ . As for decreased sunshine hours, previous results have shown that the globe radiation (sunshine hours) is the most likely cause. In the Yellow

**Table 2** Correlation between long-term mean reference evapotranspiration, pan evaporation, and related meteorological factors

Variables	Reference evapotranspiration	Pan evaporation
Relative humidity	<u>-0.31</u>	<u>-0.56</u>
Maximum temperature	<u>0.35</u>	<u>0.322</u>
Minimum temperature	0.07	0.001
Actual hours of sunshine	<u>0.43</u>	<u>0.476</u>
Wind speed	<u>0.63</u>	<u>0.308</u>
Vapor pressure deficit	<u>0.32</u>	<u>0.449</u>
Pan evaporation	<u>0.71</u>	<u>1.00</u>

*Underlined data* have passed the statistics test with 0.05 significant levels

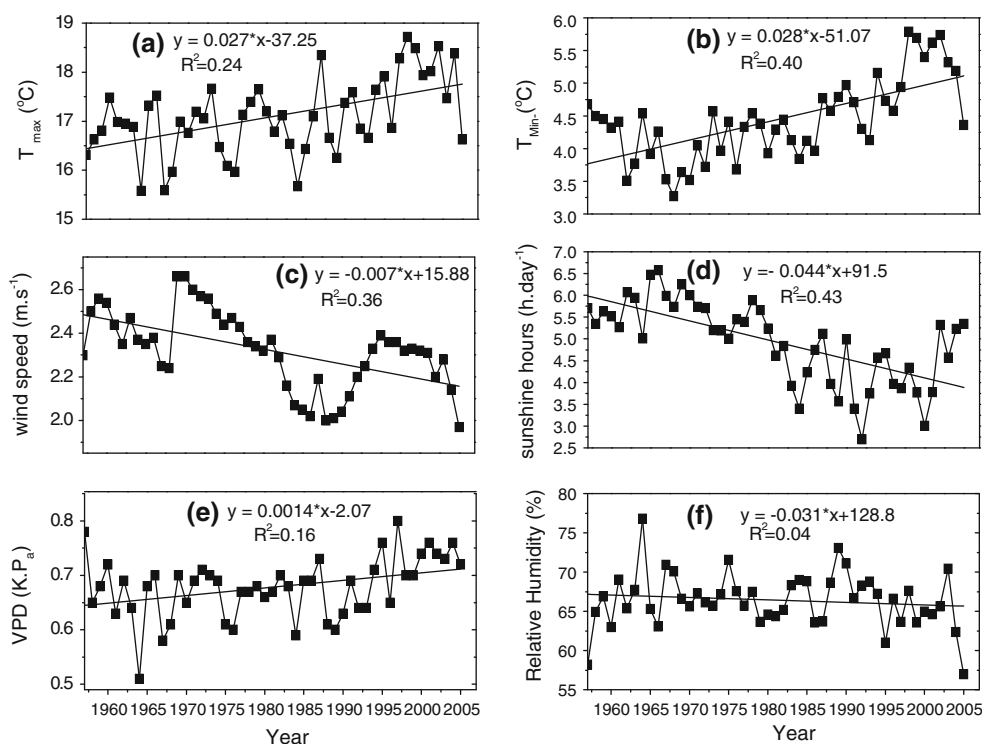
River basin, there has been many reports about the decreased trend of sunshine hours, and they speculate that aerosols may play a critical role in the decrease of solar radiation in Yellow River basin (Xu and Zhao 2005). The decreased wind speed in the Jinghe River watershed has not been discussed in the literature before. The results also show that both the maximum temperature ( $T_{max}$ ) and minimum temperature ( $T_{min}$ ) increased; however, relative humidity (RH) and diurnal temperature range (DTR) almost stayed stable. When the air temperature increased, the actual vapor pressure increased significantly (not shown in Table 3), but the slope was far less than the saturation vapor pressure (not shown in Table 3), which resulted in a significant increase of saturation vapor deficit. Finally, those variables produced a positive effect on the changes of  $ET_0$  and  $E_{pan}$ . The trend analysis shows that the reduction

**Table 3** Trends test of main meteorological factors in Jinghe River watershed (1957–2005)

No.	Variables	Unit	Parametric <i>T</i> test				Non-parameter. Mann–Kendall				
			Slope	<i>p</i> value (two-tailed)	<i>a</i>	<i>H</i> <sub>0</sub>	Kendall's tau	Statistics	<i>p</i> value (two-tailed)	<i>a</i>	<i>H</i> <sub>0</sub>
1	ET <sub>0</sub>	mm	−1.71	0.043	0.05	R	−0.138	−154.0	0.035	0.05	R
2	ET <sub>pan</sub>	mm	−4.39	0.003	0.05	R	−0.304	−341.0	0.002	0.05	R
3	T <sub>max</sub>	°C	0.03	<0.0001	0.05	R	0.312	351.0	0.002	0.05	R
4	T <sub>min</sub>	°C	0.03	<0.0001	0.05	R	0.474	533.0	<0.0001	0.05	R
5	DTR	°C	2.2E−4	0.567	0.05	N.R	−0.108	−122.0	0.282	0.05	N.R
6	Wind speed	m.s <sup>−1</sup>	−0.01	<0.0001	0.05	R	−0.449	−503.0	<0.0001	0.05	R
7	RH	%	−0.031	0.108	0.05	N.R	−0.114	−129.0	0.255	0.05	N.R
8	Sun hours	h	−0.04	<0.0001	0.05	R	−0.495	−557.0	<0.0001	0.05	R
9	VPD	KP <sub>a</sub>	1.1E−3	0.001	0.05	R	0.312	343.0	0.002	0.05	R

*H*<sub>0</sub> there is no trend in the series, *R* refuse *H*<sub>0</sub>, N.R accept *H*<sub>0</sub>, *a* = 5% significance

**Fig. 4** Time series (1957–2006) of meteorological variables over Jinghe River watershed. **a** Maximum air temperature (°C). **b** Minimum air temperature (°C). **c** Wind speed (m s<sup>−1</sup>). **d** Sunshine hours (h). **e** Saturated vapor pressure (KP<sub>a</sub>). **f** Relative humidity (%)



of wind speeds and sunshine hours were responsible factors for the reduction of ET<sub>0</sub> and ET<sub>pan</sub>.

### 3.3 Analysis of the causes of the decrease in reference evapotranspiration

In order to quantify the contributions of net radiation and wind speed to the decreasing trend of reference evapotranspiration, three scenarios were set: scenario 1: Wind speed did not decrease while other variables remained in the original trend. Scenario 2: Net solar radiation did not decrease while the other variables stayed in the same trend. Scenario 3: Both wind speed and net radiation did not

decrease while other parameters stayed in the same trend. Under these scenarios, we recalculated the ET<sub>0</sub> and compared it to the original ET<sub>0</sub> in order to detect the effects caused by the trend of variables. The following steps are performed: 1. Using the DFA method to get rid of the decreasing trend existing in wind speed and net radiation (*R*<sub>n</sub>) to make them as a trendless time series named DFA-wind and DFA-*R*<sub>n</sub>, respectively; 2. The ET<sub>0</sub> were recalculated in scenario 1 and scenario 2 by using, in each time, DFA-wind or DFA-*R*<sub>n</sub> and original data for other variables; 3. Recalculating the ET<sub>0</sub> in scenario 3 by using DFA-wind and DFA-*R*<sub>n</sub> in the same time and original data for others; 4. Finally, comparing the result with the original ET<sub>0</sub> and

the difference is considered as the influence of the trend caused by that variable. As shown in Fig. 5, the difference is remarkable between original  $ET_0$  and recalculated  $ET_0$  with DFA-wind (scenario 1) and smaller but remarkable difference is obtained between original  $ET_0$  and recalculated  $ET_0$  with DFA- $R_n$  (scenario 2). In addition, the largest difference is obtained under scenario 3. The results indicate that the solar radiation and wind speed have the decisive and dominant role in  $ET_0$  reduction.

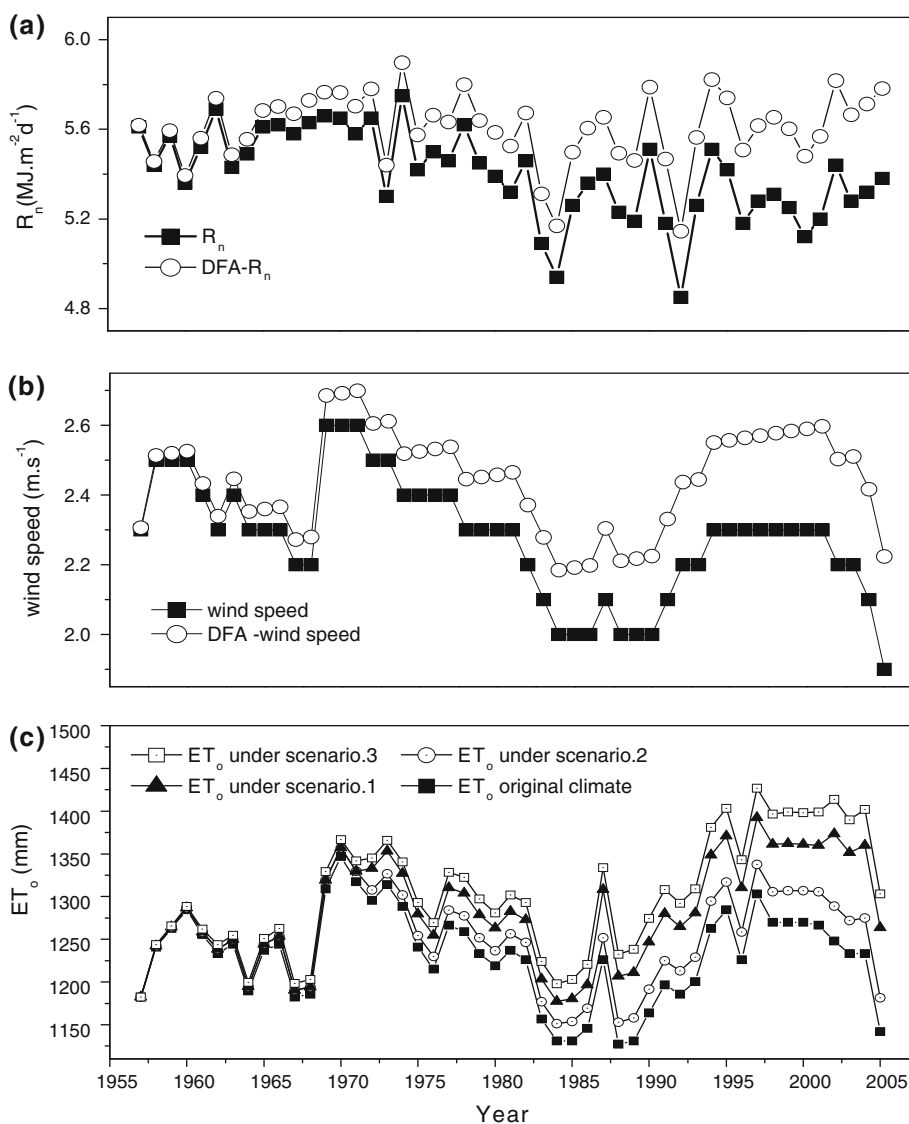
The contribution from the wind speed and net radiation were calculated by using the difference of  $ET_0$  under scenario 1 and scenario 2 divided by the difference under scenario 3, respectively. As shown in Fig. 6, the decreased  $ET_0$  caused by reduction of wind speed and net solar radiation mainly occurred after 1985, and the maximum amount reached 168 mm in 2004. The contribution from wind speed is increased from 50 to 76.21%. In contrast, the

contribution of net radiation decreased from 50 to 23.89%, and those trends were more obvious after 1985.

### 3.4 Sensitivity analysis of reference evapotranspiration to meteorological factors

In order to make the mechanism of changes of  $ET_0$  more clear, sensitivity analysis (SA) was conducted. SA is the study of how the variation (uncertainty) in the output of a mathematical model can be apportioned, qualitatively or quantitatively, to different sources of variation in the input of a model (Saltelli and Ratto 2008). In this study, nine scenarios are generated for each meteorological factor using the following equations:  $X(t) = x(t) + \Delta x$   $\Delta x = 0, \pm 5\%, \pm 10\%, \pm 15\%, \pm 20\%$  of  $x(t)$ , where  $x$  is meteorological variable,  $t$  is time in months.  $\Delta x$ , scenario step. Figure 7 shows the results of the sensitivity study. It is seen

**Fig. 5** The plot of the original annual values and the recovered stationary series for **a** net radiation (DFA- $R_n$ ) and **b** wind speed (DFA-wind), **c** the comparison of the original mean annual reference evapotranspiration with the reference evapotranspiration under three climate scenarios. Scenario 1: The dashed line with triangles is the reference evapotranspiration calculated by using DFA-wind data and original data for other variables; scenario 2: The dashed line with triangles is the reference evapotranspiration calculated by using the DFA- $R_n$  and original data for other variables. Scenario 3: Dashed line with diamonds is the reference evapotranspiration calculated by using DFA-wind and the DFA- $R_n$  and original data for other variables. The solid line with squares at the bottom is the reference evapotranspiration calculated by using original data for all meteorological variables



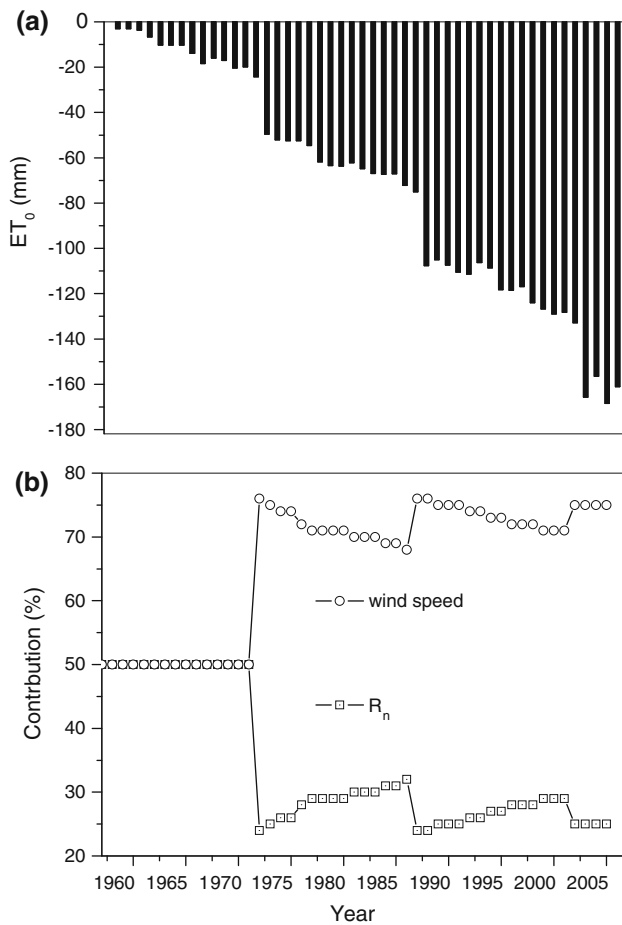


**Fig. 6** **a** The deduced amount of  $ET_0$  because of wind speed and net radiation reduction during 1957–2005. **b** The changes of annual contribution to reduction of  $ET_0$  from wind speed and net radiation ( $R_n$ ) during 1957–2005 in the Jinghe River watershed

that the sensitivity of meteorological variables to  $ET_0$  is decreased in turn from relative humidity, maximum temperature, wind speed, and net solar radiation and minimum temperature. The combination of Fig. 7 and Table 3 explain the results in Fig. 5. On one hand, the decreasing trend in wind speed is strongest among those five variables (Table 3), and it is also the high sensitive variables. Thus, its contribution to the decreasing trend of  $ET_0$  is much larger than that from the net total radiation (Fig. 5). Relative humidity is the most sensitive variable; it has no contribution to the decreasing trend in  $ET_0$  because of its temporal constancy (Table 3). The maximum temperature is highly sensitive to changes of  $ET_0$  and increasing significantly, which produced negative contribution to the decreasing trend in  $ET_0$ , which implies that negative contribution to the decreasing trend in  $ET_0$  has been offset by the positive effect from the decreasing of wind speed and solar radiation. Therefore, the decreasing trend in wind speed is the main cause of the decreasing trend in  $ET_0$

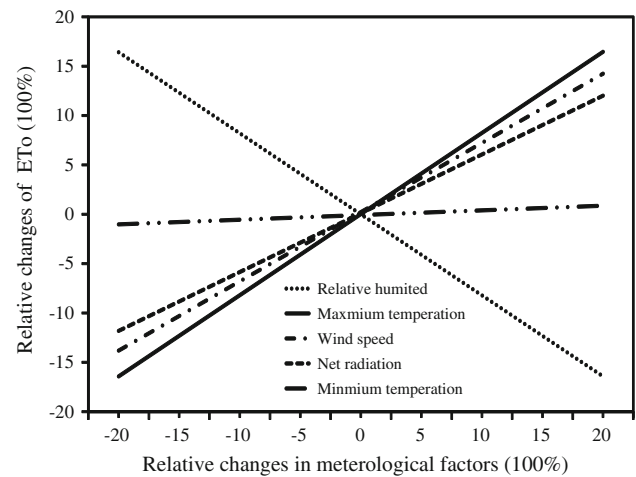


**Fig. 7** Sensitivity analysis of reference evapotranspiration to main meteorological factors

because it is not only one of the highly sensitive variables but also a variable with significant decreasing trend (Fig. 4; Table 3).

#### 4 Discussion and conclusions

Our study shows that  $ET_0$  and  $ET_{pan}$  decreased significantly during 1957–2005 in Jinghe River watershed. The change speed is  $-40.9$  mm/10 years and  $-17.7$  mm/10 years, respectively. Our analysis shows that the reductions of wind speed and sunshine hours were responsible for the reduction of  $ET_0$  and  $ET_{pan}$ . The decrease of  $ET_0$  is mainly caused by wind speed reduction because of its high sensitivity and significant decreasing trend, to a less extent by decreasing in the net solar radiation over the catchment. The contribution from wind speed to decreased  $ET_0$  increased from 50 to 76.1% during the past 49 years. Relative humidity is the most sensitive variable responding to the change of  $ET_0$ . However, its effects to  $ET_0$  change were neglected because of its insignificant changes. The positive contribution of water vapor pressure deficit to  $ET_0$ , which mainly resulted from the maximum temperature increasing, is offset by the negative effect of wind speed and net radiation reduction.

The primary reason for changes of  $ET_0$  in 14 stations varied with wind speed and sunshine hours. It is interesting to note that the contribution from wind speed to decreased  $ET_0$  in the arid area (three stations) is larger than humid area (two stations) and that result from larger decreased trend of net radiation in humid area. For the Xi'an and Bao'Ji stations, the wind speed did not have an obvious downtrend, but an uptrend. Although there was a larger reduction in net solar radiation (compare to arid and semi-



arid region), it is not strong enough to compensate the positive contribution to  $ET_0$  caused by increasing in wind speed and temperature. Therefore, it is reasonable that both the  $ET_0$  and  $ET_{pan}$  in Xi'an and Bao'ji stations had a slight increase trend.

**Acknowledgments** We acknowledge, with gratitude, the financial support from the National Natural Science Foundation of China (30972421) and the National Basic Research Program of China (2009CB421308). We also the Professor D. Y. Gong (Beijing Normal University) for his valuable advice and to China Meteorological Administration for providing meteorological data.

## References

- Abakumova GM et al (1996) Evaluation of long-term changes in radiation, cloudiness, and surface temperature on the territory of the former Soviet Union. *J Clim* 9:1319–1327
- Allen RG, Pereira LS, Raes D, Smith M (1998) Crop evapotranspiration. Guidelines for computing crop water requirements. FAO Irrigation and drainage paper 56, Rome
- Bunde A, Havlin S, Kantelhardt JW, Penzel T, Peter JH, Voigt K (2000) Correlated & uncorrelated regions in heart-rate fluctuations during sleep. *Phys Rev Lett* 85(17):3736–3739
- Burn DH, Hesch NM (2007) Trends in evaporation for the Canadian prairies. *J Hydrol* 336(1–2):61–73
- Chattopadhyay N, Hulme M (1997) Evaporation and potential evapotranspiration in India under conditions of recent and future climate change. *Agric For Meteorol* 87:55–73
- Chen R, Ersi K, Yang J, Lu S, Zhao W (2004) Validation of five global radiation models with measured daily data in China. *Energy Convers Manage* 45(11–12):1759–1769
- Dai A, Tenberth KE, Karl TR (1999) Effects of clouds, soil moisture, precipitation and water vapor on diurnal temperature range. *J Clim* 12:2451–2473
- Golubev VS et al (2001) Evaporation changes over the contiguous United States and the former USSR: a reassessment. *Geophys Res Lett* 28:2665–2668
- Gong L, Xu C, Chen D, Halldin S, Chen Y (2006) Sensitivity of the Penman-Monteith reference evapotranspiration to key climatic variables in the Changjiang (Yangtze River) basin. *J Hydrol* 329(3–4):620–629
- Harbeck E (1962) A practical and field technique for measuring reservoir evaporation utilizing mass-transfer theory. *Geol Surv Prof Pap Wash* 272(E):100–105
- Helsel D, Hirsch R (1993) Statistical methods in water resources. Elsevier, Amsterdam
- Hobbins MT, Ramirez JA, Brown TC (2004) Trends in pan evaporation and actual evapotranspiration across the conterminous U.S.: paradoxical or complementary? *Geophys Res Lett* 31:L13503. doi:10.1002/2004GL019846
- Kaiser DP, Qian Y (2002) Decreasing trends in sunshine duration over China for 1954–1998: indication of increased haze pollution? *Geophys Res Lett* 29(21):2042
- Kantelhardt J, Koscielny-Bunde E, Rego H, Havlin S, Bunde A (2001) Detecting long-range correlations with detrended fluctuation analysis. *Phys A Stat Mech Appl* 295(3–4):441–454
- Kendall M (1975) Rank correlation measures. Charles Griffin, London
- Koscielny-Bunde E, Kantelhardt J, Braun P, Bound A, Havlin S (2006) Long-term persistence and multifractality of river runoff records: detrended fluctuation studies. *J Hydrol* 322(1–4):120–137
- Liepert BG (2002) Observed reductions of surface solar radiation at sites in the United States, worldwide from 1961 to 1990. *Geophys Res Lett* 29:1421. doi:10.1029/2002GL014910
- Liepert BG, Feichter J, Lohmann U, Roeckner E (2004) Can aerosols spin down the water cycle in a warmer and moister world? *Geophys Res Lett* 31:L06207. doi:10.1029/2003GL019060
- Liu CM, Zeng Y (2004) Changes of pan evaporation in the recent 40 years in the Yellow River basin. *Water Int* 29(4):510–516
- Liu Q, Yang ZF, Cui BS, Sun T (2010) The temporal trends of reference evapotranspiration and its sensitivity to key meteorological variables in the Yellow River Basin, China. *Hydrol Process* 24(15):2171–2181
- Mann H (1945) Nonparametric tests against trend. *Econometrica* 13(3):245–259
- Paturel J, Servat E, Vassiliadis A (1995) Sensitivity of conceptual rainfall-runoff algorithms to errors in input data—case of the GR2 M model. *J Hydrol* 168(1–4):111–125
- Peterson TC, Golubev VS, Groisman PY (1995) Evaporation losing its strength. *Nature* 377:687–688
- Prescott JA (1940) Evaporation from a water surface in relation to solar radiation. *T Roy Soc South Aust* 64:114–125
- Qian T et al (2006) Simulation of global land surface conditions from 1948–2004. Pt I: forcing data and evaluations. *J Hydrometeorol* 7:953–975
- Qiu GY, Yano T, Momii K (1998) An improved methodology to measure evaporation from bare soil based on comparison of surface temperature with a dry soil surface. *J Hydrol* 210(1–4):93–105
- Qiu GY, Yin J, Xiong YJ, Zhao SH, Wang P (2008) Studies on the effects of climatic warming-drying trend and land use change on the runoff in the Jinghe River basin. *J Nat Res* 23(2):211–218 (In Chinese)
- Roderick ML, Farquhar GD (2004) Changes in Australian pan evaporation from 1970–2002. *Int J Climatol* 24:1077–1090
- Roderick ML, Farquhar GD (2005) Changes in New Zealand pan evaporation since the 1970s. *Int J Climatol* 25:2031–2039
- Saltelli A, Ratto M (2008) Global sensitivity analysis: the primer. Wiley, New York
- Shenbin C, Yunfeng L, Thomas A (2006) Climatic change on the Tibetan Plateau: potential evapotranspiration trends from 1961–2000. *Clim Change* 76(3):291–319
- Sumner DM, Jacobs JM (2005) Utility of Penman-Monteith, Priestley-Taylor, reference evapotranspiration, and pan evaporation methods to estimate pasture evapotranspiration. *J Hydrol* 308(1–4):81–104
- Tebakari T, Yoshitani J, Suvanpimol C (2005) Time-space trend analysis in pan evaporation over Kingdom of Thailand. *J Hydrol Eng* 10:205–216
- Thornthwaite C (1948) An approach toward a rational classification of climate: the geographical review. *New York* 38:55–94
- Turc L (1961) Estimation des besoins en eau d'irrigation, evapotranspiration potentielle, formule climatique simplifiée et mise a jour. *Ann Agron* 12(1):13–49
- Xu CY, Singh VP (2000) Evaluation and generalization of radiation-based methods for calculating evaporation. *Hydrol Process* 14(2):339–349
- Xu CY, Singh VP (2001) Evaluation and generalization of temperature-based methods for calculating evaporation. *Hydrol Process* 15(2):305–319
- Xu CY, Vandewiele G (1994) Sensitivity of monthly rainfall-runoff models to input errors and data lengths. *Hydrol Sci J* 39(2):157–176
- Xu CY, Gong LB, Jiang T, Chen DL, Singh VP (2006) Analysis of spatial distribution and temporal trend of reference

- evapotranspiration and pan evaporation in Changjiang (Yangtze River) catchment. *J Hydrol* 327(1–2):81–93
- Xu ZX, Zhao F (2005) Variation of sunlight radiation duration in the Yellow River Basin. *Resour Sci* 27(5):153–160 (in Chinese)
- Yin Y, Wu S, Chen G, Dai E (2009) Attribution analyses of potential evapotranspiration changes in China since the 1960s. *Theor App Climatol* 101(1–2):19–28